Heliyon 10 (2024) e29827

Contents lists available at ScienceDirect

Heliyon

journal homepage: www.cell.com/heliyon

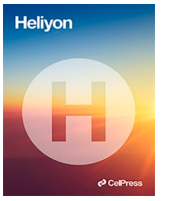

Research article

Establishment of glioma prognosis nomogram based on the function of meox1 in promoting the progression of cancer

Peng Pan [a,1], Aiping Guo [b,1], Lu Peng [c,*]

[a] Department of clinical Laboratory, Nanjing Stomatological Hospital, Affiliated Hospital of Medical School, Nanjing University, Nanjing, China
[b] Department of Medical Oncology, Luhe People's Hospital, Nanjing, China
[c] Department of clinical laboratory, Nanjing Brain Hospital, Affiliated Brain Hospital of Nanjing Medical University, Nanjing, China

ARTICLE INFO

Keywords:
Glioma
Prognosis
Bioinformatics
Meox1

ABSTRACT

Background: Gliomas stand out as highly predominant malignant nervous tumors and are linked to adverse treatment outcomes and short survival periods. Current treatment options are limited, emphasizing the need to identify effective therapeutic targets. The heterogeneity of tumors necessitates a personalized treatment approach with an effective grouping system. Meox1 has been implicated in promoting tumor progression in diverse cancers; nonetheless, its role in gliomas remains unelucidated.

Material/methods: **Utilized immunohistochemistry** to assess the expression of Meox1 protein in glioma tissues. Proliferation and invasion assays were conducted on wild-type and meox1-overexpressed glioma cells using the CCK8 and Transwell assays, respectively. The expression levels of meox1 and its related genes in gliomas were obtained from Chinese Glioma Genome Atlas (CGGA), along with the corresponding patient survival periods. LASSO regression modeling was employed to construct a scoring system for patients with gliomas, categorizing them into high-/low-risk groups. Additionally, a nomogram for predicting the survival period of patients with glioma was developed using multivariate logistic analysis.

Results: We attempted, for the first time, to demonstrate heightened expression of Meox1 in glioma tumor tissues, correlating with significantly increased invasion and proliferation abilities of glioma cells following meox1 overexpression. The scoring system effectively stratified patients with glioma into high-/low-risk groups, revealing differences in the survival period and immunotherapy efficacy between the two groups. The integration of this scoring system with other clinical indicators yielded a nomogram capable of effectively predicting the survival period of individuals with gliomas.

Conclusions: Our study established a stratified investigation system based on the levels of meox1 and its related genes, providing a novel, cost-effective model for facilitating the prognosis prediction of individuals with glioma.

1. Introduction

Primary central nervous system tumors originate in the human central nervous system [1]. Among these, gliomas are the most

* Corresponding author.
E-mail addresses: jerry0727@163.com (P. Pan), 929813607@qq.com (A. Guo), pl_0710@njmu.edu.cn (L. Peng).
[1] Equal first author.

https://doi.org/10.1016/j.heliyon.2024.e29827
Received 6 January 2024; Received in revised form 15 April 2024; Accepted 16 April 2024
Available online 24 April 2024

prevalent and malignant, with diffuse gliomas being particularly aggressive [1]. According to the World Health Organization, gliomas are classified into four distinct grades. (I, II, III, and IV) based on malignancy level, tumor atypia, and mitotic activity [2]. Although the primary treatment for gliomas involves extensive surgical resection followed by adjuvant chemotherapy and radiotherapy, the outcomes often remain unsatisfactory [3]. The median survival time for grades I-II(low-grade) glioma is 12 years, while that for grades III-IV (high-grade) glioma is approximately 1 year [4,5]. The mutation status of isocitrate dehydrogenase (IDH) is closely linked to the prognosis of patients, and MGMT methylation was considered an important prognostic biomarker [6,7]. These studies suggest that glioma treatment largely depends on molecular diagnosis and classification [8]. The identification of new and effective treatment targets is an urgent issue in current glioma research.

The homeobox gene family includes transcription factors that control the embryonic development of mammals, including humans, such as Mesenchyme homeobox 1 (Meox1) [9]. Meox1 is critically involved in the regulation of muscle and bone development [10]. In recent years, with advancements in tumor research, researchers have discovered that Meox1 is linked to the onset and progression of various human tumors. In these tumors, Meox1 promotes tumor occurrence and development through different pathways [11,12]. For example, Meox1 is overexpressed in hepatocellular carcinoma tissues. It reprograms Treg cells, leading to a decrease in $CD4^+$ T cell content in the tumor microenvironment [13]. There are currently no reports on Meox1 in glioma, however, its homologous factor, Meox2, has been found to promote glioma cell proliferation through the ERK/MAPK and PI3K/AKT pathways. Additionally, Meox2 protein methylation promotes IDH mutations [14]. Given their homologous nature, Meox1 and Meox2 may exert similar effects in gliomas.

Our study revealed elevated Meox1 expression in glioma patient tissues, which was found to enhance the proliferation and migration of glioma cells. Simultaneously, bioinformatics analysis website GEPIA2 was utilized to analyze the variance in survival across patients with glioma showing high-/low-expression of meox1. Further, the GEPIA2 website was utilized to predict the 30 most relevant genes for Meox1 expression (Meox1-related genes, MRGs) and multivariate Cox regression analysis was employed to determine the six MRGs most relevant to glioma prognosis (H2AFX, EYA3, SIX1, MEOX1, NOG, and LDLR). Based on this, we developed a nomogram to predict the prognosis of gliomas. Overall, the acquired data implies that the expression levels of six MRGs and the nomogram can predict overall production rate of patients with glioma, providing novel targets for the prevention, diagnosis of neuroglioma and new ideas for its research.

2. Materials and methods

2.1. Data collection and sample acquisition

Herein, the gene expression and the clinical details of individuals with glioma were acquired from the mRNAseq_325 dataset of the Chinese Glioma Genome Atlas (CGGA) (http://www.cgga.org.cn/), and clinical data are presented in Supplementary Table 1. Gene mutation datas of patient with glioma were selected from the information accessed at The Cancer Genome Atlas Program (https://portal.gdc.cancer.gov/). The prediction of Meox1-related genes using Gene Expression Profiling Interactive Analysis (GEPIA2, http://gepia2.cancer-pku.cn) and GSE4290 data from Gene Expression Omnibus (GEO, https://www.ncbi.nlm.nih.gov/geo/) were selected to comparative assessment of meox1 expression levels between glioma patient tissues and normal brain tissues. The overall survival rate comparison between high-/low-level meox1 patients was performed using the GEPIA2 website. The pathological specimens of patients with glioma used in this study were obtained from the Affiliated Brain Hospital of Nanjing Medical University. The study protocol underwent review by the Ethics Committee of the Affiliated Brain Hospital of Nanjing Medical University and was given approval (NO.2022-KY184-01).

2.2. Immunohistochemistry

Tissue samples were fixed in 4 % polyformaldehyde for 3–4 h, then dehydrated in ascending ethanol concentrations (75 % for 1.5 h, 95 % for 3 h, absolute for 2.5 h), and finally cleared in xylene (No. 1 and No. 2, each for 30 min). Subsequently, the tissues were embedded, sectioned, and mounted. The dewaxed tissues were hydrated at room temperature, circled using an immunohistochemical pen, and blocked with goat serum. A Meox1 primary antibody (Abcam) was introduced to cover the tissue, with subsequent overnight incubation in a wet box at 4 °C. Following this, the secondary antibody (from Abcam) was added at a volume of 50 μl, and 100 μl of DAB solution was then applied to each slide. Ultimately, the tissues were examined and photographed using a microscope.

2.3. Cell culture

The cells were acquired from the American Type Culture Collection (ATCC) and identified by Procell Life Science&Technology Co., Ltd (Wuhan, China). U251 (RRID:CVCL_0021) and U87 (RRID:CVCL_0022) cells were cultured in DMEM complete medium (from Gibco) comprising 10 % fetal bovine serum, in a 5 % CO_2 incubator at 37 °C. The medium was changed every 24 h, and the cells were passaged at a ratio of 1:2 or 1:3 when cell confluence reached approximately 85 % and the cells reached the logarithmic growth phase.

2.4. Cell transfection

The overexpression plasmid vector was constructed by Guangzhou Ruibo Co. Prior to transfection, the cell density was determined to be approximately 30%–50 %. Following the digestion of the cells with trypsin, a uniform single-cell suspension was prepared. After

counting, cells inoculated in a new plate, and complete medium was introduced into each well. The new plate was placed in a 5 % CO_2 incubator,37 °C, and transfection was completed within 24 h. Then, 5 μL of plasmid was added to serum-free MEM medium without antibiotics, mixed well. Mixed the two solutions for 20 min, 26 °C. Then, 2 ml of the prepared transfection solution was introduced into plate, mixed well, 6 h (37 °C, 5 % CO_2).

2.5. Cell proliferation assay (CCK8)

Using the CCK8 kit from Beyotime, the glioma cell suspension (100μL/well) was inoculated in a 96-well plate with subsequent pre-culturing in an incubator (37 °C, 5 % CO_2). Subsequently, CCK solution (10 μL) was introduced into each well, and incubation of the culture plate was carried out for 1–4 h, avoiding light. The optical density at a wavelength of 450 nm was quantified utilizing an enzyme-linked immunosorbent assay (ELISA) methodology.

2.6. Cell invasion assay (Transwell)

Using the Transwell® kit from Corning, 100 μL of diluted Matrigel matrix gel was added to each Transwell chamber. The cell suspension was taken and 200 μL was introduced into each chamber. A total volume of 600 μL of Dulbecco's Modified Eagle Medium (DMEM), supplemented with 10 % fetal bovine serum, was added to each compartment of a 24-well plate. The plate was then incubated at 37 °C under a 5 % carbon dioxide atmosphere for a duration of 24 h. Subsequently, the cells were fixed by transferring the plate to a new 24-well plate with 600 μL of methanol in each well. Following fixation, the plate was further processed by moving it to another 24-well plate, where each well contained 600 μL of crystal violet staining solution for cell staining. Transwell chamber was removed, observed, and recorded using an inverted microscope.

2.7. Gene identification and expression analysis

The 30 genes most closely related to Meox1 were predicted using the GEPIA2 website. The expression of all MRGs in the glioma dataset, mRNAseq_325, was obtained from the CGGA website.

2.8. Mutation analysis

The tumor mutation burden (TBM) was determined according to the number of mutations per million bases to determine MRG mutation status. Genetic mutation information for 508 individuals was retrieved from the TCGA database.

2.9. Immunotherapy response prediction and patient classification

The Tumor Immune Dysfunction and Exclusion (TIDE) tool (http://tide.dfci.harvard.edu) was utilized to calculate a range of previously identified transcriptomic biomarkers. This was done by analyzing the gene expression data of glioma patients, aiming to forecast their responsiveness to immunotherapeutic treatments [15]. Patients with glioma were categorized using various classification methods. The classifications included age (<50 years old and ≥50 years old), sex (male and female), WHO grades (I-II and III-IV), IDH status (IDH-mutant and IDH-wild type), and neuroglioma type (primary neuroglioma, recurrent neuroglioma, and secondary neuroglioma).

2.10. Determination of prognostic-related genes and patients' risk scores

Univariate Cox regression analysis was utilized to identify the significant genes. Subsequently, LASSO regression modeling was utilized to select the most useful prognostic marker genes, and tenfold cross-validation was used to examine the prime value of the parameter λ. Univariate prognostic analyses were conducted for several genes. In the multivariate logistic regression analysis, variables with a p-value below 0.05 were selected to identify the factors associated with the prognosis of glioma patients. LASSO Cox regression analysis was used to identify genes with the smallest error in risk characteristics among the 30 MRGs. The patient risk score was obtained by multiplying the expression of the obtained gene by the corresponding coefficient. High- and low-risk patients were classified per the median scores of all patients.

The patients were randomly divided into training (n = 155) and test (n = 156) cohorts at a 1:1 ratio. The difference in overall survival (OS) between the high-/low-risk groups was tested using the training group, test group, and all samples.

2.11. Multivariate Prognostic Analysis

Using Cox regression analyses, including both univariate and multivariate approaches, risk, risk score, age, sex, grade, and histology were used to perform independent and joint survival prediction analyses. The objective was to observe the effect of each factor and their combination on the prognosis of the patient and to obtain the risk ratio of each factor in the Multivariate Prognostic Analysis. This ratio represents the change in the patient's risk of death for each additional unit of a certain factor when other factors are the same.

2.12. Nomogram establishment

Nomograms have been established based on risk scores and related risk factors to predict the prognosis of gliomas [16]. A nomogram is a graphical prediction model that intuitively displays the relationships between multiple predictive factors and prognostic results. In the nomogram, each predictor has a corresponding fractional axis, and each patient factor is scored on the fractional axis according to its specific value. The scores for all factors are then added up to obtain the total score. The effectiveness of the prediction was examined using the c-index and the relevant calibration curve. This comprehensive approach allowed for a more accurate prediction of patient outcomes.

2.13. Statistical analysis

R software (v 4.3.1) was used to analyze the data. The independent *t*-test was used to compare continuous data obtained from the cell invasion and proliferation experiments, while the log-rank test was used to compare OS data of patients in different groups. $P < 0.05$ (two-sided) was considered statistically significant.

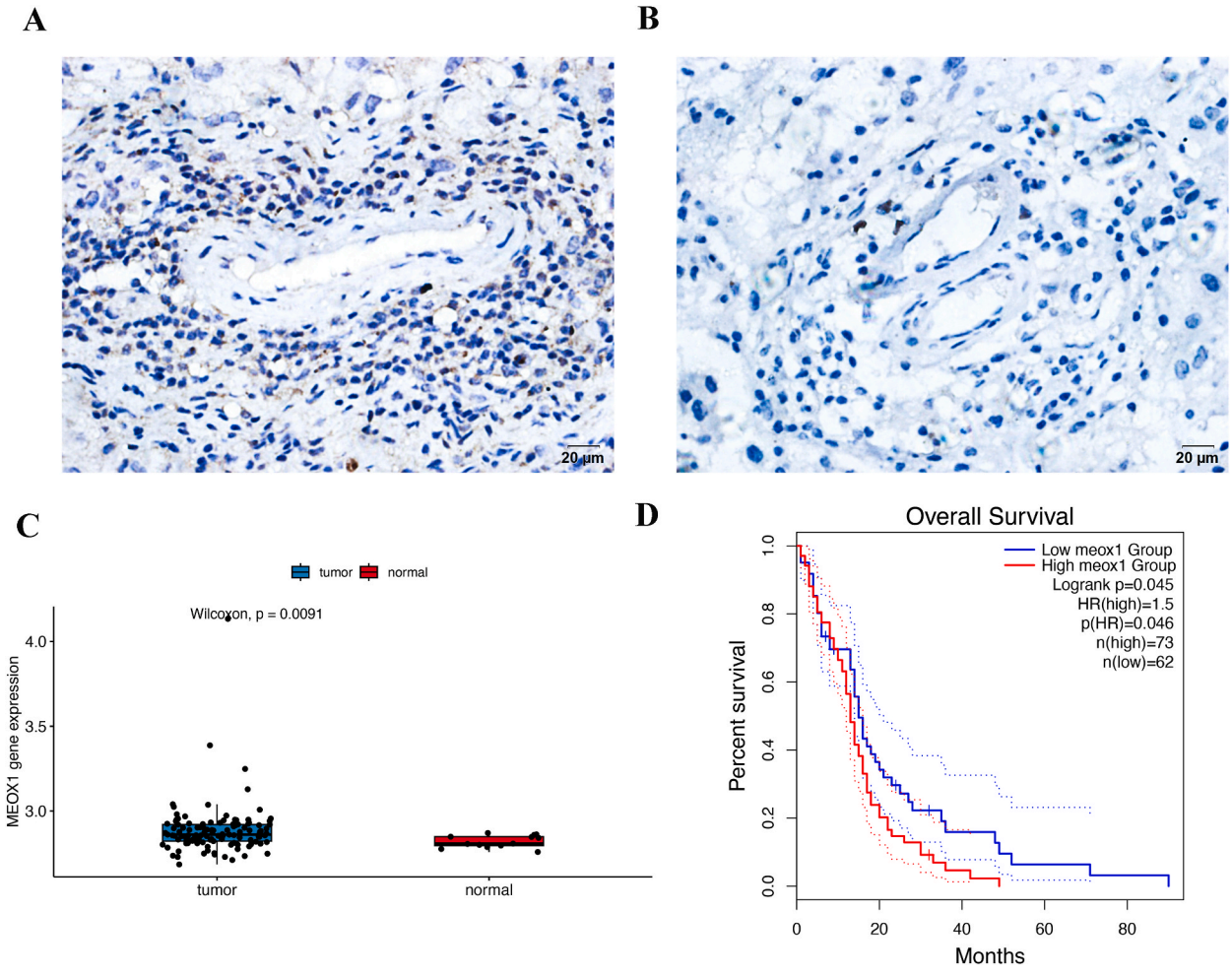

Fig. 1. Expression of Meox1 in glioma tissues and its relationship with glioma occurrence and prognosis. (A) Expression of the Meox1 protein in tumor tissues and (B) surrounding tissues of glioma patients. (C) The meox1 mRNA expression in glioma tissues is higher than that in normal brain tissues in the GEO database (n = 180, $P = 0.0091$). (D) Glioma patients with elevated expression of Meox1 have a lower survival period than those with reduced expression of Meox1. The blue line is the Low Meox1 Group (n = 62), and the red line is the High Meox1 Group (n = 73), $P = 0.046$. (For interpretation of the references to color in this figure legend, the reader is referred to the Web version of this article.)

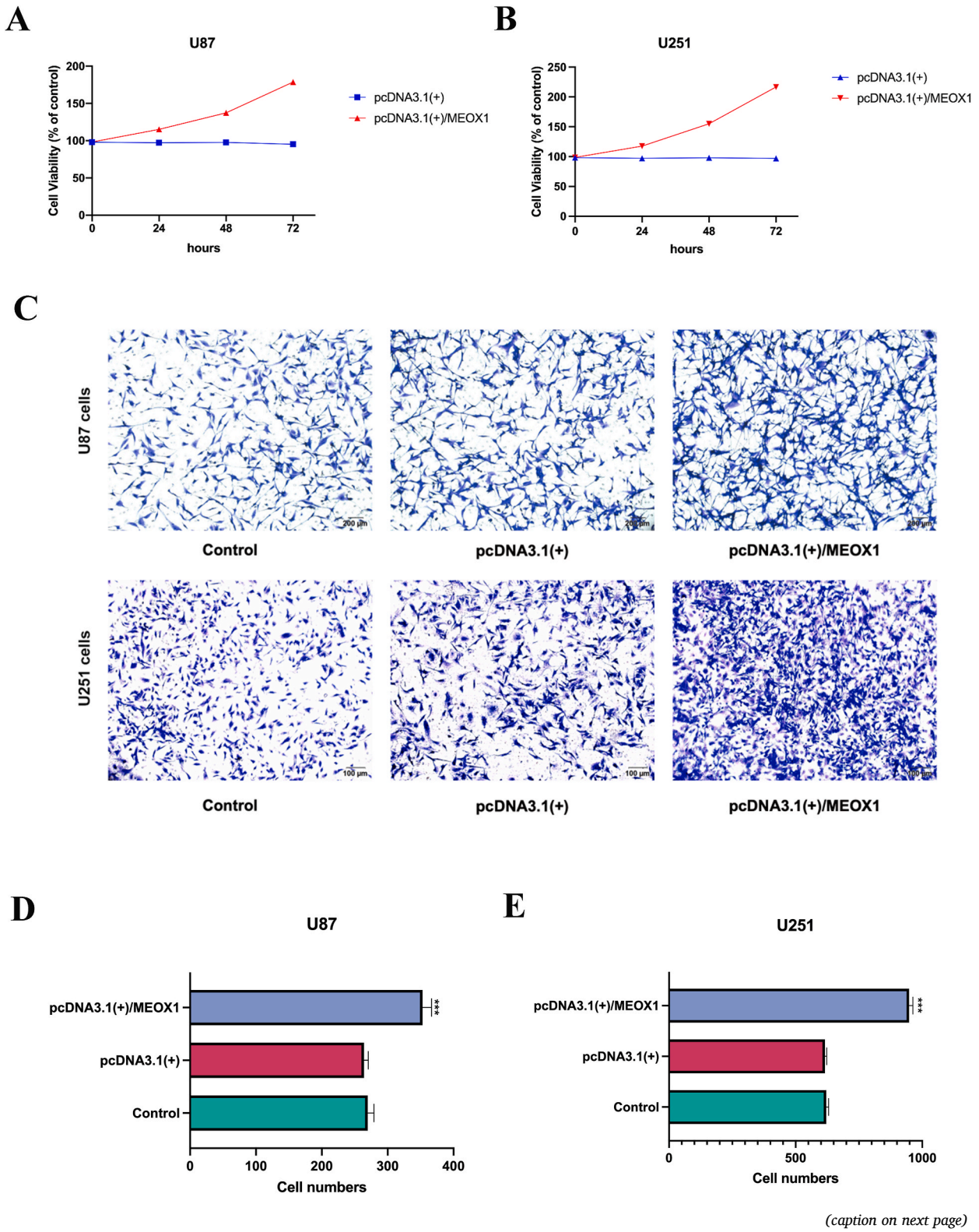

(caption on next page)

Fig. 2. Meox1 enhances the proliferative and invasive capabilities of glioma cells. (A) CCK8 assay verified that after overexpression of pcDNA3.1+/meox1 plasmid, U87 cell proliferation was faster than pcDNA3.1+ (n = 3). (B) CCK8 assay verified that after overexpression of pcDNA3.1+/meox1 plasmid, U251 cell proliferation was faster than pcDNA3.1+. (C) Images of cell invasion after expressing blank plasmid (control), pcDNA3.1+ plasmid, and pcDNA3.1+/meox1 plasmid in U251 and U87 cells. (D) & (E) Transwell cell detection demonstrated that in U251 and U87 cells overexpressing pcDNA3.1+/meox1 plasmid, relative to the control and pcDNA3.1+ as the control group, the number of invading tumor cells increased in the meox1 overexpression group (n = 3). ***$P < 0.001$.

3. Results

3.1. Expression of Meox1 in neuroglioma tissues and its correlation with OS

In glioma patient tissues, immunohistochemical analysis revealed that the Meox1 protein was expressed in tumor tissues with a wide distribution range (Fig. 1A–B). Statistical analysis of the GSE4290 dataset from the GEO database showed that meox1 exhibited heightened expression in tumor samples compared to non-tumor samples ($p = 0.0091$) (Fig. 1C). Additionally, the OS of patients in the high meox1 expression group was shorter ($p = 0.045$) (Fig. 1D).

3.2. Meox1 promotes the proliferation and invasion of glioma cells

After transfection of U87 and U251 cells with pcDNA3.1+/meox1+ plasmid and pcDNA3.1+ plasmid, the cell numbers were compared with those of the blank control group and presented as mean ± SD. In U87 cells, the cell numbers after 24 h were 97.25 % ± 0.94 % and 115.2 % ± 1.67 % ($p = 0.002$), after 48 h were 97.78 % ± 0.73 % and 137.5 % ± 0.81 % ($p < 0.0001$), and after 72 h were 95.30 % ± 1.03 % and 178.8 % ± 1.62 % ($p < 0.0001$) respectively. In U251 cells, the cell numbers after 24 h were 97.21 % ± 0.28 % and 117.7 % ± 0.96 % ($p < 0.0001$), after 48 h were 98.01 % ± 0.58 % and 155.2 % ± 0.945 % ($p < 0.0001$), and after 72 h were 96.99 % ± 0.64 % and 216.8 % ± 0.61 % ($p < 0.0001$) respectively (Fig. 2A–B). We found that the control group, pcDNA3.1+ group, and pcDNA3.1+/meox1+ overexpression group of U87 cells had 24-h invasive cells of 269.7 ± 9.45, 264.0 ± 6.56, and 353.0 ± 13.53, respectively. The pcDNA3.1+/meox1+ overexpression group had a significant difference in the number of invasive cells in comparison to the control group and pcDNA3.1+ group ($p = 0.0009$ and $p = 0.0005$). The control group, pcDNA3.1+ group, and pcDNA3.1+/meox1+ overexpression group of U251 cells had 24-h invasive cells of 620.7 ± 9.45, 615.7 ± 7.02, and 948.0 ± 14.80, respectively. The pcDNA3. +/meox1+ overexpression group exhibited a significant difference in the number of invasive cells in comparison to the control group and pcDNA3.1+ group ($p < 0.0001$ and $p < 0.0001$) (Fig. 2C–E).

3.3. Assessing the expression profiles and mutation patterns of meox1 and its related genes in glioma

The expression profiles of all the MRGs in the glioma dataset mRNAseq_325, obtained from the CGGA website, are shown in Fig. 3A. Genetic mutation data for these genes obtained from TCGA revealed that 92 patients exhibited mutations in MRGs, with specific genes (ATM, LRP6, ATP2A1, EYA4, GNF3, DHRS7C, LDLR, LRP5, TBX6, FSD2, NBN, SIX4, TBX18, KRT24, EYA3, WNT8B, ENO3, and CDH17) exhibiting a maximum mutation frequency of 3 %. However, no mutations were observed in the remaining genes. Missense mutations were the most prevalent ones (Fig. 3B).

3.4. Determining prognostic-related MRGs and developing risk assessment formulas

In the CGGA dataset, univariate prognostic analysis revealed that H2AFX, EYA4, EYA3, EYA2, SIX1, TBX18, MEOX2, MEOX1, TCF15, MIXL1, and LRP5 are positively correlated with survival, whereas ATM, PAX1, TBX6, NOG, WNT1, LDLR, and WNT8B are negatively correlated with survival (Fig. 4A). LASSO Cox regression analysis confirmed that among the 30 MRGs, H2AFX, EYA3, SIX1, MEOX1, NOG, and LDLR exhibited the smallest errors in risk characteristics (Fig. 4B–C). Relative risk scores for patients are listed in Table 1.

3.5. Differences in survival duration and MRG gene expression among glioma patients across different risk groups

The CGGA dataset was categorized into high-(n = 155) and low-risk (n = 158) groups on the basis of the expression levels of six genes (H2AFX, EYA3, SIX1, MEOX1, NOG, and LDLR). Remarkably, the number of patients who survived with high-risk glioma was considerably lower in comparison to those having low-risk glioma. In the training cohort, tissues from high-risk patients demonstrated elevated expression levels of H2AFX, EYA3, SIX1, and MEOX1, whereas tissues of low-risk individuals showed heightened expression levels of NOG and LDLR (Fig. 5A). This pattern was consistently observed not only in the test cohort but also across all samples (Fig. 5B–C).

3.6. Predicting OS and immunotherapy efficacy in individuals having low and high-risk glioma

A substantial variation in OS was evident between both risk categories in all samples, training group, and test group ($p < 0.001$ for all) (Fig. 6A–C). The TIDE score of high-risk patients was considerably less than that of low-risk patients ($p < 0.0001$) (Fig. 6D),

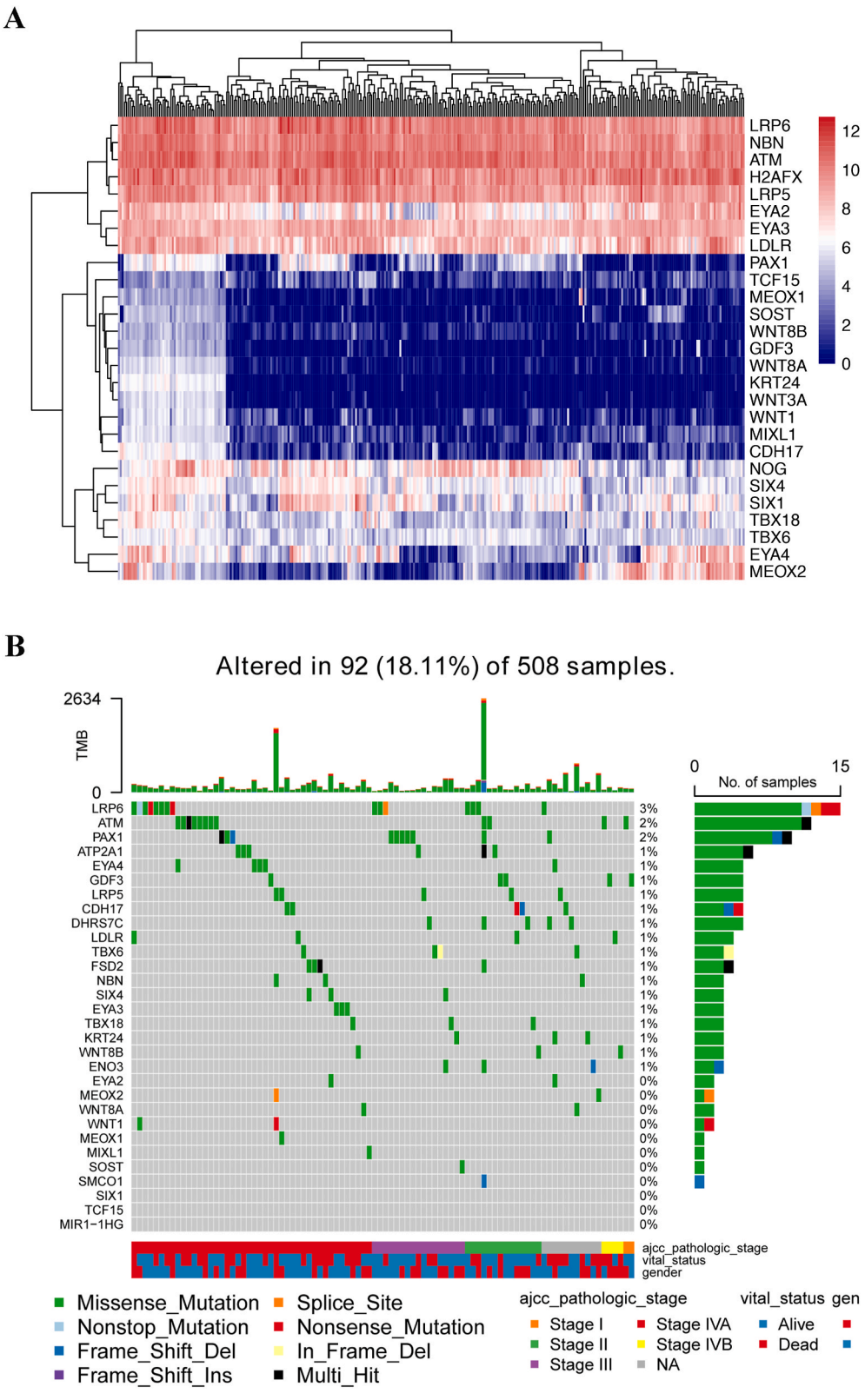

(caption on next page)

Fig. 3. Expression and mutation of genes in glioma associated with Meox1. (A) The expression of Meox1-associated genes in the CGGA glioma dataset mRNAseq_325. (B) Mutation of Meox1-related genes in the TCGA glioma dataset. Different colors were used to represent different patient statuses (survival/death), mutation status, and disease pathological grading among a total of 508 samples. (For interpretation of the references to color in this figure legend, the reader is referred to the Web version of this article.)

indicating that the high-risk individuals may exhibit increased resistance to tumor immunotherapy.

3.7. Kaplan-Meier curves depicting OS for distinct types of glioma patients within high/low-risk groups

Differences in OS were observed within different risk groups. OS exhibited significant differences between the aforementioned risk groups in both age groups ($\geq$50 years: n = 87, $p < 0.001$; <50 years: n = 226, $p < 0.001$) (Fig. 7A–B). Both male and female individuals in the high-risk group exhibited substantially reduced OS relative to those in the low-risk group (male: n = 197, $p < 0.001$; female: n = 116, $p < 0.001$) (Fig. 7C–D). Among individuals experiencing WHO grade III-IV gliomas, the high-risk group depicted considerably lower OS compared to that of the other group (n = 211, $p < 0.001$) (Fig. 7E–F). A substantial variation in OS between both risk groups was observed in IDH-mutant and IDH-wild-type patients (IDH-mutant: n = 168, $p < 0.001$; IDH-wild-type: n = 145, $p < 0.001$) (Fig. 7G–H). Additionally, a substantial difference in OS was found between the two risk groups across all three types of patients (n = 226, $p < 0.001$ for primary cancer; n = 58, $p = 0.014$ for recurrent; and n = 29, $p = 0.026$ for secondary cancer) (Fig. 7I–K).

3.8. Prognostic nomogram

Univariate Cox analysis showed that age, risk score, grade, and histology were independently linked to the glioma patients' prognosis. However, sex showed no correlation (Fig. 8A). Multivariate analysis demonstrated that only the grade and risk score were related to the prognosis (Fig. 8B).

In the receiver operating characteristic (ROC) analysis, the model depicted good prognostic ability. The AUC values of the ROC curves for risk score, age, sex, grade, and histology were 0.780, 0.602, 0.481, 0.758, and 0.706, respectively (Fig. 8C). Among the parameters evaluated, the risk score obtained from the MRG-based risk model demonstrated the highest AUC, making it the most predictive factor. The ROC curves for one, three, and five years showed AUCs of 0.780, 0.863, and 0.896, respectively, all indicating high predictive values (Fig. 8D).

Fig. 9A illustrates an example of utilizing the nomogram for the prediction of the survival probability of a patient. The Nomogram shows all prognostic correlation factors along with their total score. The image describes a 38-year-old woman with low-risk, G2 glioma. The cumulative score of various risk factors amounts to 121 points. The one-, three-, and five-year survival rates are predicted as 94.1 %, 84 %, and 76.7 %, respectively. The C-index of the risk score was the highest and had the greatest predictive effect (Fig. 9B). The calibration curve closely matched the ideal curve, suggesting the strong predictive ability of the model (Fig. 9C).

4. Discussion

Glioma, the most prevalent malignant primary nervous system tumor, presents a significant challenge to the global public health system, with around 20,000 novel cases documented in the United States every year [17]. Research has revealed substantial individual heterogeneity among patients with gliomas, necessitating precise prediction and tailored treatment [18]. The integration of prognosis-related genes with traditional clinical parameters, including grade and histology, may yield more accurate outcomes than single biomarkers.

Meox1, a homologous-domain transcription factor, exerts crucial involvement in mammalian cell development and differentiation. Ongoing research aims to elucidate its function in tumors. This study is the first to identify the differential expression of the Meox1 protein in glioma compared to adjacent tissues and to confirm its involvement in enhancing the proliferative and invasive behaviors of tumor cells in glioma.

These findings are consistent with observations regarding the role of Meox1 in other tumor types. Decreased Meox1 expression in breast cancer was observed to reduce the number of cancer stem cells and tumor cells. In ovarian cancer, Meox1 promotes tumor development by fostering tumor cell proliferation, migration, and invasion via PBX1 [12,19].

The outcomes of this study depicted that Meox1 exerts a similar impact on gliomas by promoting the proliferative and invasive capacities of tumor cells. Bioinformatic analysis demonstrated a significant elevation in Meox1 expression levels in glioma tumor tissues relative to the normal tissues. Furthermore, patients exhibiting high Meox1 expression experienced significantly lower OS than those exhibiting low Meox1 expression. This suggests that Meox1 exerts an influence on glioma progression and pathogenesis, significantly impacting patient survival.

Throughout tumor development, genes function in a network, each fulfilling distinct roles. These genes are interconnected, mutually influential, and collectively promote tumor progression [20]. The studies in recent years have predominantly focused on the functions of gene groups and their predictive value for tumor treatment outcomes. For instance, the expression levels of gene groups comprising ACTN1, ESR2, CCND1, MYB, and PKM can predict the efficacy of radiotherapy. Similarly, the gene groups consisting of CSE1L, CSTB, MTHFR, DAGLA, MMP10, and GYS2 can effectively predict the prognosis of hepatocellular carcinoma [21,22].

Based on our previous observation that Meox1 exerts a crucial influence on glioma progression and pathogenesis, 30 genes were selected that may interact with Meox1 and are expressed in gliomas. Using LASSO regression analysis, expression levels of gene clusters

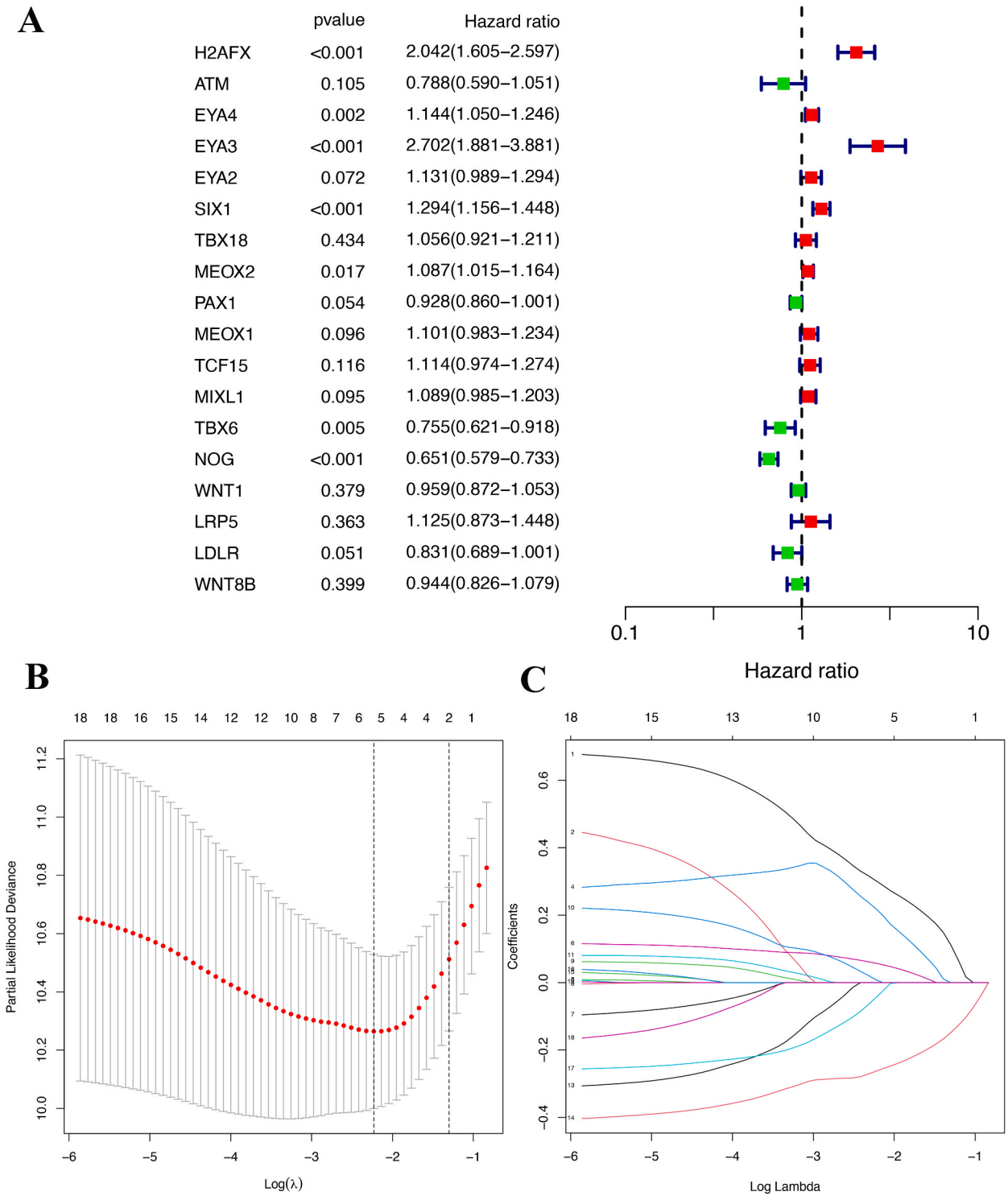

Fig. 4. Discovery and selection of genes related to the prognosis. (A) Univariate Cox analysis was utilized to identify prognosis-associated genes. (B) Tenfold cross-validation for tuning parameter selection in the LASSO model. (C) LASSO coefficient profiles of 18 prognostic MRGs for glioma.

were combined with patient outcomes to establish an MRG model. This model included H2AFX, EYA3, SIX1, MEOX1, NOG, and LDLR as a glioma prognosis prediction system. Our MRG glioma prognosis prediction model accurately assessed patient prognosis, revealing a substantial variation in survival period between low-/high-risk patients ($p < 0.01$). Moreover, by merely detecting the expression levels, this prediction model accurately determined the one-, three-, and five-year survival rates of glioma patients. This approach can

Table 1
The relative value of the patient risk score and gene expression.

Gene name	coef
H2AFX	0.469940238733383
EYA3	0.48642466132904
SIX1	0.113717194589953
MEOX1	0.160572545074172
NOG	−0.375462431134804
LDLR	−0.28326051045571

save substantial funds and medical resources compared to previous whole-genome detection methods.

Among the selected MRGs, H2AFX exerts a significant influence on DNA repair, replication, and chromosomal stability. Additionally, it can promote tumor cell development by regulating tumor immunity. H2AFX can serve as a prognostic marker for hepatocellular carcinoma [23–25]. EYA3, a member of the Haloacid Dehalogenase (HAD) family, primarily functions in protein phosphorylation. In colorectal cancer, the EYA3-SIX5-p300 complex is involved in tumor pathogenesis through the mediation of EGFR/VEGFD/MMPs. Conversely, in breast cancer, it upregulates PD-L1 to promote immune cell apoptosis, thus shortening the survival period of patients [26–28]. SIX1, a significant regulator of mammalian organ development and disease occurrence, exhibits a critical influence on the progression of most tumors. It can promote the onset of many tumors, encompassinglung cancer, hepatocellular carcinoma, and prostate cancer. Moreover, enhanced expression of SIX1 is correlated with a shortened survival period [29–31]. NOG can antagonize the tumor-promoting effect of BMP in glioma, and its low expression may contribute to treatment resistance in these patients [32,33]. LDLR, an LDL receptor, when upregulated in gliomas, can promote the uptake of exogenous LDL cholesterol by tumor cells. This leads to the further deposition of cholesterol in lysosomes and subsequent death of GBM cells [34]. In this study, H2AFX, EYA3, SIX1, and MEOX1 exhibited a negative correlation with the OS and promoted tumor progression. Conversely, NOG and LDLR inhibited tumor development and showed a positive correlation with OS in glioma patients. These findings align with prior studies, providing further validation for the accuracy of our results.

The TIDE score is a metric employed to predict the efficacy of tumor immunotherapy, primarily relying on two key immune evasion mechanisms: immune dysfunction and immune exclusion [15]. Our findings indicated that low-risk patients exhibited elevated TIDE scores in comparison to those in high-risk group. This proposes low-risk tumors demonstrate increased responsiveness to immunotherapy. Additionally, the need for further investigation of the involved specific mechanisms is highlighted by the differences in genes associated with immune cell function between the two patient groups. This underscores the potential of leveraging immune-based interventions to manage tumors within this subgroup, paving the way for promising avenues for further exploration.

As per the assessed literature, the integration of this MRG prognostic model and the nomogram is a novel approach in glioma research, potentially serving as an effective tool for assessing glioma prognosis and disease grading. Utilizing mutation data from the TCGA database, it was discovered that the MRGs in this study generally did not exhibit gene mutations during the onset of glioma. This finding further substantiates the likelihood that the genes in this cluster perform biological functions as intact genes, thereby excluding the influence of gene mutations on glioma progression.

Practically, the six MRGs were more likely to undergo routine testing because of their ability to reduce the need for whole-genome testing. The nomogram, which combines the MRG with sex, age, histology, and grade, effectively predicts the survival rate of glioma patients. This confirms that a combination of clinical indicators and gene testing can effectively address the substantial individual heterogeneity of gliomas.

However, the limitations of this study warrant further investigation. Primarily, these research data were predominantly sourced from the CGGA database and the patients were of Asian descent. Therefore, the application of these findings to other races should be approached with caution, and further experimental verification is necessary. Additionally, further validation is required for the expression and prognostic impact of MRGs at the protein level. Moreover, since the nomogram is based on a retrospective study design, prospective clinical trials are necessary for further verification.

Despite these limitations, a key advantage of this nomogram is the simplification of the readily accessible and assessable parameters. This suggests that this model holds promise for clinical applications, supporting personalized assessments of the expected survival rates of patients with gliomas. Furthermore, it can function as a stratification tool for clinical research, providing evidence for early interventions aimed at enhancing OS rates in the context of glioma.

5. Conclusions

While Meox1 is known to facilitate the advancement of multiple cancer types, its involvement in the context of gliomas remains unexplored in literature. This study is the first to identify the expression of Meox1 in gliomas and elucidate its function in enhancing tumor cell proliferation and invasion. Furthermore, six genes related to Meox1 were identified that have been implicated in tumor development. Using data analysis from the CGGA database, a nomogram was developed that effectively predicts the survival period and immunotherapeutic efficacy in glioma patients. In conclusion, this research offers a novel perspective on the treatment of gliomas.

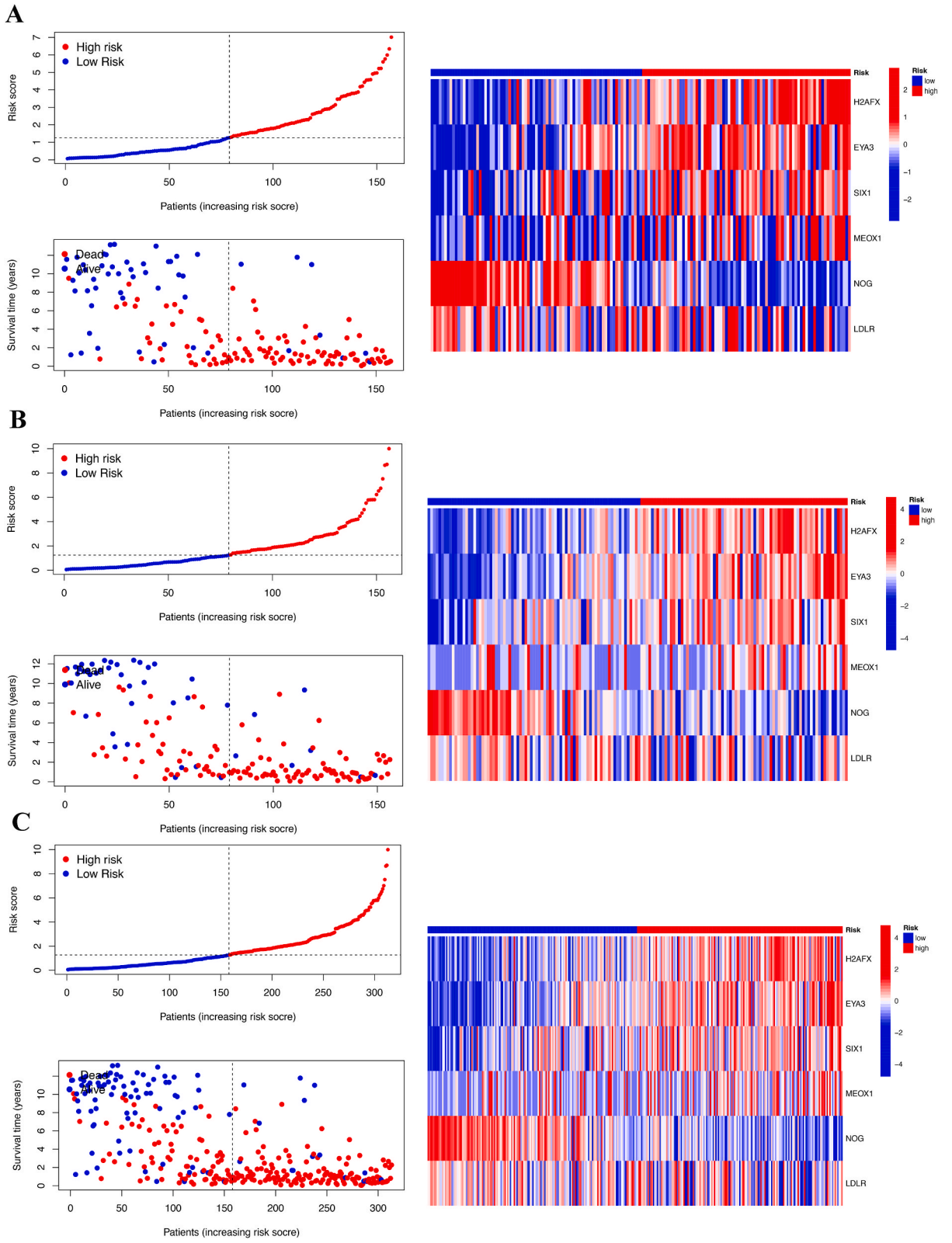

Fig. 5. Survival status and MRG expression of low-risk and high-risk glioma patients. (A) Survival status and MRG expression of glioma patients from both risk categories in the training cohort. (B) Survival status and MRG expression of two risk group patients in the test cohort. (C) Survival status and MRG expression of all patients from aforementioned groups.

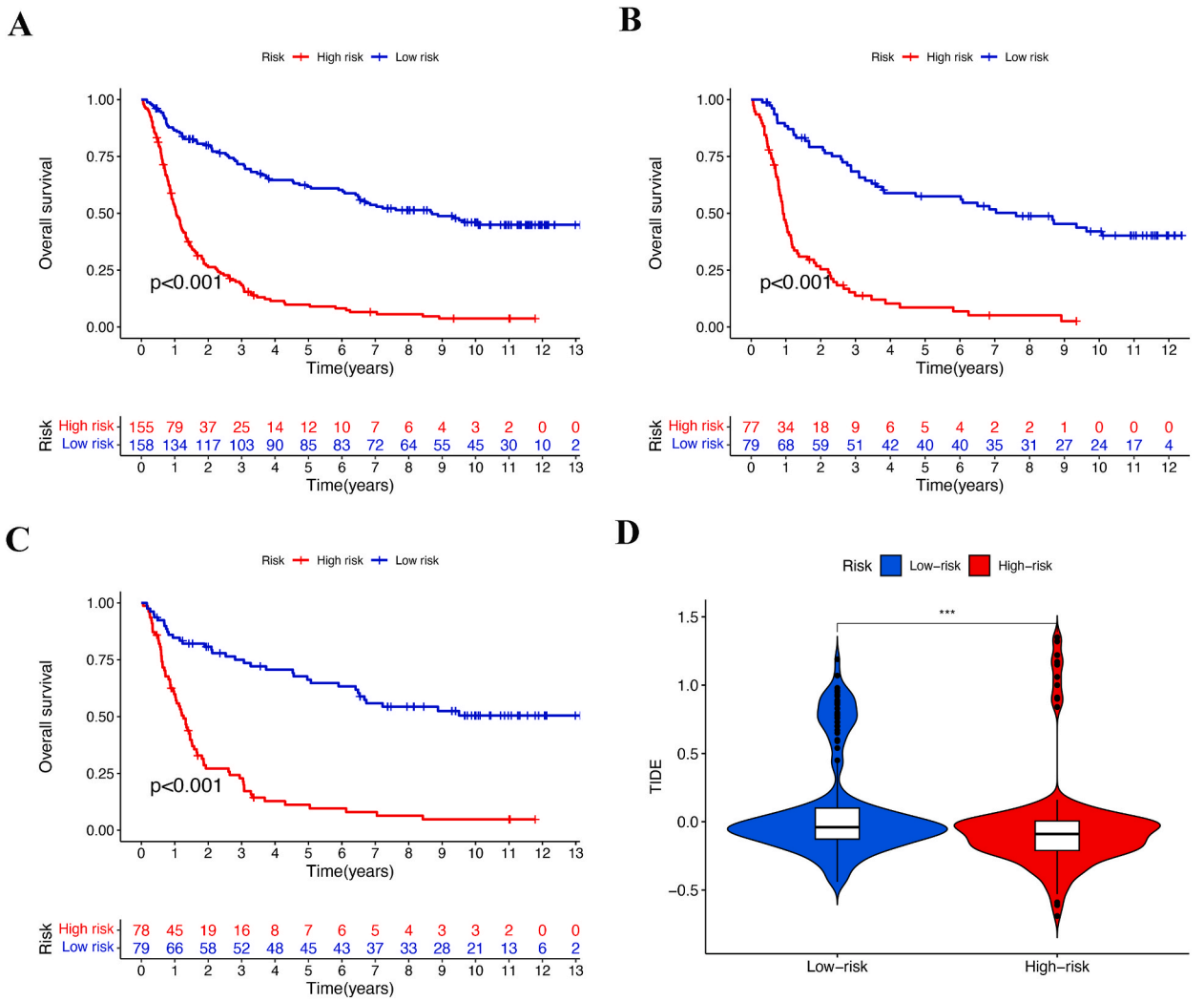

Fig. 6. Survival period and TIDE score of patients with high-risk and low-risk glioma. (A) Survival period of patients from both risk groups in the training group (n = 156). (B) Survival period of patients from two risk categories in the test group (n = 157). (C) Survival period of all patients from two risk groups (n = 313). (D) The difference in TIDE scores between patients of both risk groups. ***$P < 0.001$.

Ethics statement

The study "Establishment of glioma prognosis nomogram based on the function of meox1 in promoting the progression of cancer", which research by Laboratory Department of the Affiliated Brain Hospital of Nanjing Medical University, was approved by the Ethics Committee of the Affiliated Brain Hospital of Nanjing Medical University (NO. 2022-KY184-01), conformed to the ethical standards for medical research involving human subjects, as laid out in the 1964 Declaration of Helsinki and its later amendments. The research period is from 2022.08.06 to 2024.12.31. Informed consent was waived because of the retrospective nature of this study.

Funding

None.

Consent for publication

All authors agree with the publication of this manuscript. This manuscript has not been published and is not under consideration for publication elsewhere.

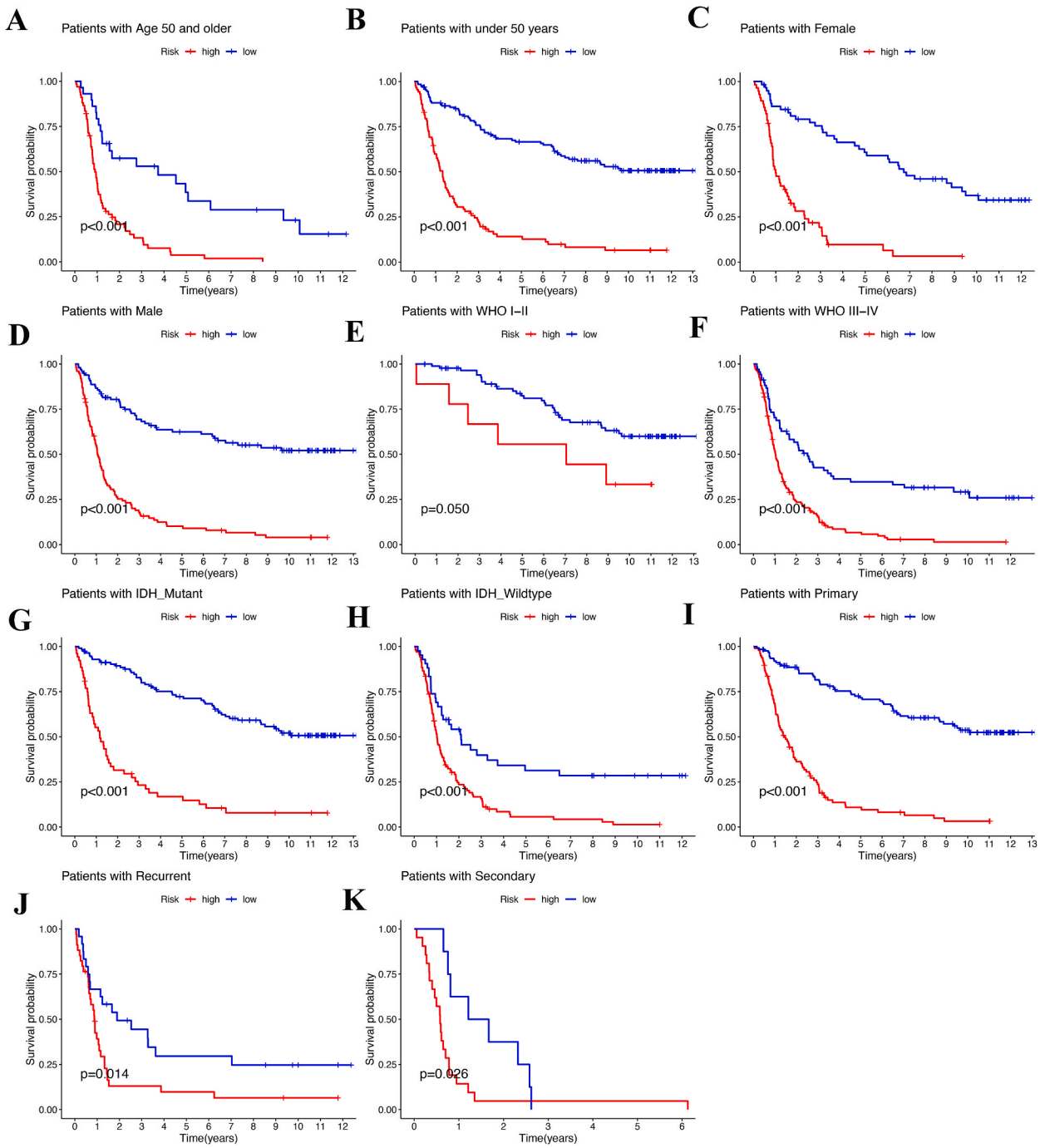

Fig. 7. Differences in survival period between patients with high-risk and low-risk glioma in different categories. (A) Survival period of patients from two risk groups (age ≥50, n = 87). (B) Survival period of individuals from the aforementioned risk groups (age <50, n = 226). (C) Survival period of female patients from two risk groups (n = 116). (D) Survival period of male patients from two groups (n = 197). (E) The survival variation between patients from aforementioned groups of WHO I-II grade glioma (n = 102). (F) The disparity in survival between patients from the above-mentioned groups of WHO III-IV grade glioma (n = 211). (G) Survival period of IDH mutant individuals from both risk groups (n = 168). (H) Survival period of IDH-wild-type patients from both risk groups (n = 145). (I) Survival period of individuals with primary high-risk and low-risk glioma (n = 226). (J) Survival period of patients experiencing recurrent high-risk and low-risk glioma (n = 58). (K) Survival period of individuals with secondary high-risk and low-risk glioma (n = 29).

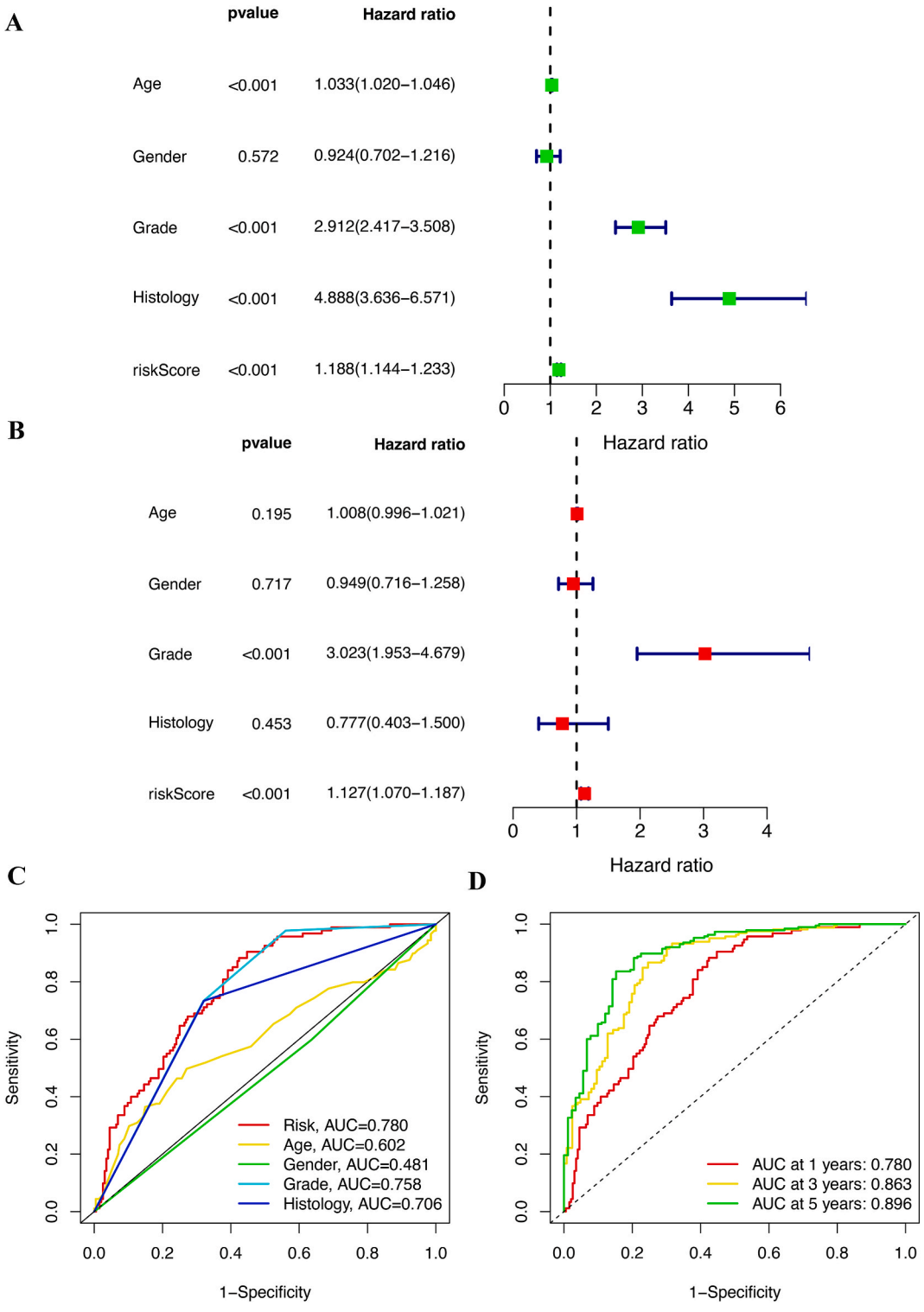

Fig. 8. Regression analyses (univariate and multivariate) and ROC of risk score and clinical factors in every sample. (A) Univariate and (B) Multivariate Cox analysis depict the impacts of age, sex, grade histology, and risk score in all cohorts. (C) The ROC for age, risk, sex, histology, and grade with OS for glioma cohorts. (D) ROC curves depicted the predictive efficiency of the risk score for glioma cohorts in 1-, 3-, and 5-years.

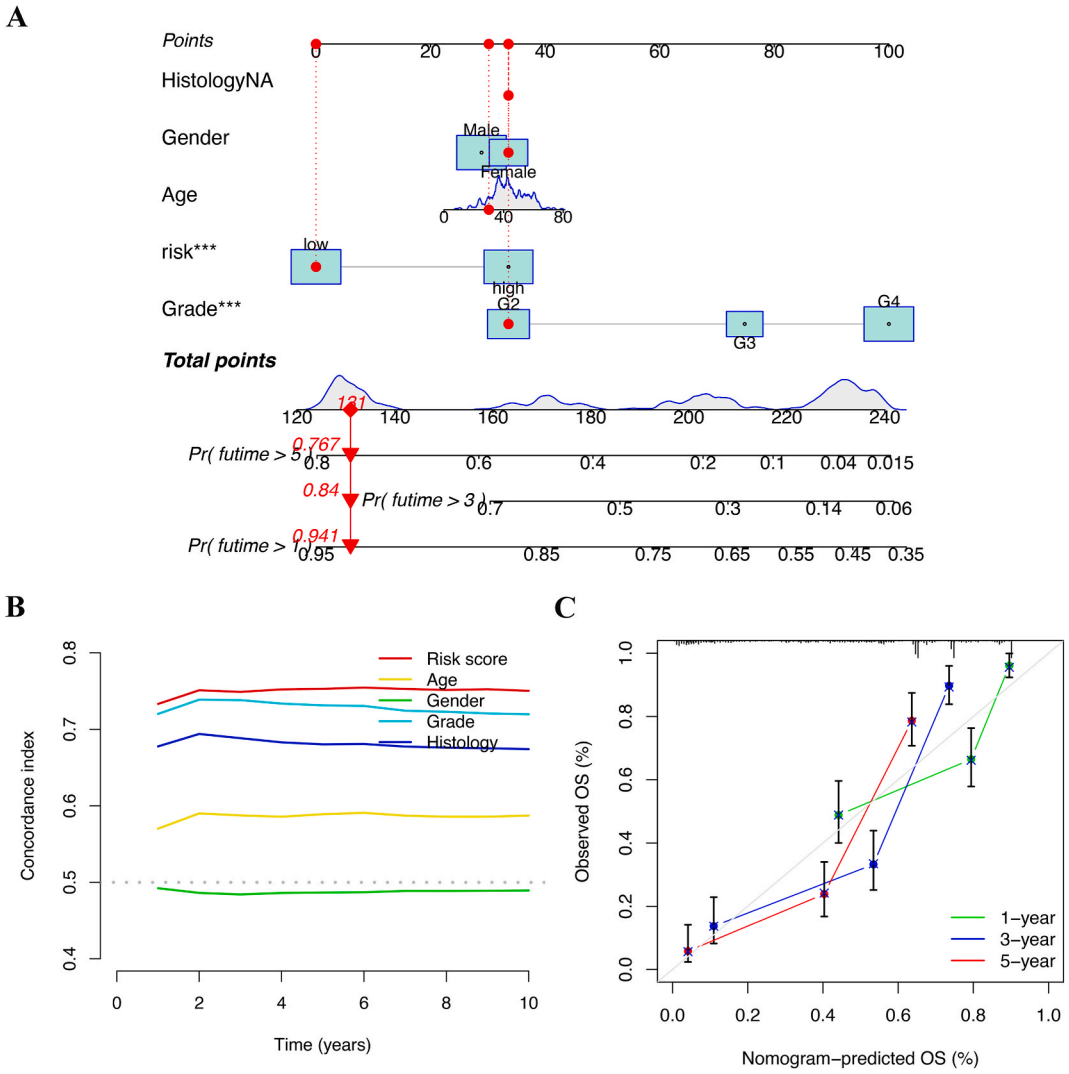

Fig. 9. Development and verification of nomogram. (A) The prediction of OS risk in patients with glioma by the nomogram. (B) C-index of risk score and clinical parameters. (C) Relevant calibration curve of the nomogram.

Availability of data and materials

The authors confirm that all supporting data for this study are available within the article and its supplementary materials. All data are available for readers to review and use.

CRediT authorship contribution statement

Peng Pan: Writing – original draft, Supervision, Software, Methodology, Funding acquisition. **Aiping Guo:** Writing – original draft, Visualization, Validation, Software, Methodology, Conceptualization. **Lu Peng:** Writing – review & editing, Methodology, Formal analysis, Data curation, Conceptualization.

Declaration of competing interest

The authors declare that they have no known competing financial interests or personal relationships that could have appeared to influence the work reported in this paper.

Appendix A. Supplementary data

Supplementary data to this article can be found online at https://doi.org/10.1016/j.heliyon.2024.e29827.

References

[1] J. Yue, R. Huang, Z. Lan, B. Xiao, Z. Luo, Abnormal glycosylation in glioma: related changes in biology, biomarkers and targeted therapy, Biomark. Res. 11 (1) (2023) 54.
[2] D.N. Louis, A. Perry, P. Wesseling, D.J. Brat, I.A. Cree, D. Figarella-Branger, et al., The 2021 WHO classification of tumors of the central nervous system: a summary, Neuro Oncol. 23 (8) (2021) 1231–1251.
[3] X. Liu, Q. Guo, G. Gao, Z. Cao, Z. Guan, B. Jia, et al., Exosome-transmitted circCABIN1 promotes temozolomide resistance in glioblastoma via sustaining ErbB downstream signaling, J. Nanobiotechnol. 21 (1) (2023) 45.
[4] C.J. Pachocki, E.M. Hol, Current perspectives on diffuse midline glioma and a different role for the immune microenvironment compared to glioblastoma, J. Neuroinflammation 19 (1) (2022) 276.
[5] J.G. Nicholson, H.A. Fine, Diffuse glioma heterogeneity and its therapeutic implications, Cancer Discov. 11 (3) (2021) 575–590.
[6] J.J. Miller, Targeting IDH-mutant glioma, Neurotherapeutics 19 (6) (2022) 1724–1732.
[7] O. Gusyatiner, M.E. Hegi, Glioma epigenetics: from subclassification to novel treatment options, Semin. Cancer Biol. 51 (1) (2018) 50–58.
[8] F.Y. Chiu, Y. Yen, Imaging biomarkers for clinical applications in neuro-oncology: current status and future perspectives, Biomark. Res. 11 (1) (2023) 35.
[9] K. Dong, X. Guo, W. Chen, A.C. Hsu, Q. Shao, J.F. Chen, et al., Mesenchyme homeobox 1 mediates transforming growth factor-β (TGF-β)-induced smooth muscle cell differentiation from mouse mesenchymal progenitors, J. Biol. Chem. 293 (22) (2018) 8712–8719.
[10] M.V.P. Dauer, P.D. Currie, J. Berger, Skeletal malformations of Meox1-deficient zebrafish resemble human Klippel-Feil syndrome, J. Anat. 233 (6) (2018) 687–695.
[11] L. Sun, H. Yuan, J. Burnett, M. Gasparyan, Y. Zhang, F. Zhang, et al., MEOX1 promotes tumor progression and predicts poor prognosis in human non-small-cell lung cancer, Int. J. Med. Sci. 16 (1) (2019) 68–74.
[12] M. Gasparyan, M.C. Lo, H. Jiang, C.C. Lin, D. Sun, Combined p53- and PTEN-deficiency activates expression of mesenchyme homeobox 1 (MEOX1) required for growth of triple-negative breast cancer, J. Biol. Chem. 295 (34) (2020) 12188–12202.
[13] G. Alvisi, A. Termanini, C. Soldani, F. Portale, R. Carriero, K. Pilipow, et al., Multimodal single-cell profiling of intrahepatic cholangiocarcinoma defines hyperactivated Tregs as a potential therapeutic target, J. Hepatol. 77 (5) (2022) 1359–1372.
[14] G. Tachon, K. Masliantsev, P. Rivet, A. Desette, S. Milin, E. Gueret, et al., MEOX2 transcription factor is involved in survival and Adhesion of glioma stem-like cells, Cancers 13 (23) (2021) 5943.
[15] P. Jiang, S. Gu, D. Pan, J. Fu, A. Sahu, X. Hu, et al., Signatures of T cell dysfunction and exclusion predict cancer immunotherapy response, Nat. Med. 24 (10) (2018) 1550–1558.
[16] V.P. Balachandran, M. Gonen, J.J. Smith, R.P. DeMatteo, Nomograms in oncology: more than meets the eye, Lancet Oncol. 16 (4) (2015) e173–e180.
[17] A.S. Modrek, N.S. Bayin, D.G. Placantonakis, Brain stem cells as the cell of origin in glioma, World J. Stem Cell. 6 (1) (2014) 43–52.
[18] J.G. Nicholson, H.A. Fine, Diffuse glioma heterogeneity and its therapeutic implications, Cancer Discov. 11 (3) (2021) 575–590.
[19] J. Li, Y. Sun, X. Zhi, Y. Sun, Z. Abudousalamu, Q. Lin, et al., Unraveling the molecular mechanisms of lymph node metastasis in ovarian cancer: focus on MEOX1, J. Ovarian Res. 17 (1) (2024) 61.
[20] T. Jesan, S. Sinha, Modular organization of gene-tumor association network allows identification of key molecular players in cancer, J. Biosci. 47 (2022) 60.
[21] Y.X. Yao, Z.T. Bing, L. Huang, Z.G. Huang, Y.C. Lai, A network approach to quantifying radiotherapy effect on cancer: radiosensitive gene group centrality, J. Theor. Biol. 462 (2019) 528–536.
[22] G.M. Liu, H.D. Zeng, C.Y. Zhang, J.W. Xu, Identification of a six-gene signature predicting overall survival for hepatocellular carcinoma, Cancer Cell Int. 19 (2019) 138.
[23] H. Hu, T. Zhong, S. Jiang, H2AFX might be a prognostic biomarker for hepatocellular carcinoma, Cancer Rep (Hoboken) 6 (1) (2023) e1684.
[24] J.M. Cloutier, S.K. Mahadevaiah, E. Ellnati, A. Nussenzweig, A. Tóth, J.M. Turner, Histone H2AFX links meiotic chromosome asynapsis to prophase I oocyte loss in mammals, PLoS Genet. 11 (10) (2015) e1005462.
[25] A.J. de Sousa Portilho, Silva EL. da, E.C.A. Bezerra, C.B.S. Moraes Rego Gomes, V. Ferreira, M.E.A. de Moraes, et al., 1,4-Naphthoquinone (CNN1) induces apoptosis through DNA damage and promotes upregulation of H2AFX in Leukemia multidrug resistant cell line, Int. J. Mol. Sci. 23 (15) (2022) 8105.
[26] R.L. Vartuli, H. Zhou, L. Zhang, R.K. Powers, J. Klarquist, P. Rudra, et al., Eya3 promotes breast tumor-associated immune suppression via threonine phosphatase-mediated PD-L1 upregulation, J. Clin. Invest. 128 (6) (2018) 2535–2550.
[27] K. Roychoudhury, R.S. Hegde, The eyes absent proteins: unusual HAD family tyrosine phosphatases, Int. J. Mol. Sci. 22 (8) (2021) 3825.
[28] C. Yang, H. Liu, Both a hypoxia-inducible EYA3 and a histone acetyltransferase p300 function as coactivators of SIX5 to mediate tumorigenesis and cancer progression, Ann. Transl. Med. 10 (13) (2022) 752.
[29] H.S. Zhao, X.M. Tao, Q. Wang, Y.Y. Fang, H.Y. Zhang, H.Q. Wang, et al., Silencing SIX1 by miR-7160 inhibits non-small cell lung cancer cell growth, Aging (Albany NY) 13 (6) (2021) 8055–8067.
[30] L. Lu, J. Huang, J. Mo, X. Da, Q. Li, M. Fan, et al., Exosomal lncRNA TUG1 from cancer-associated fibroblasts promotes liver cancer cell migration, invasion, and glycolysis by regulating the miR-524-5p/SIX1 axis, Cell. Mol. Biol. Lett. 27 (1) (2022) 17.
[31] Y. Liao, W. Sun, Z. Shao, Y. Liu, X. Zhong, Y. Deng, et al., A SIX1 degradation inducer blocks excessive proliferation of prostate cancer, Int. J. Biol. Sci. 18 (6) (2022) 2439–2451.
[32] G.A. Videla Richardson, C.P. Garcia, A. Roisman, I. Slavutsky, D.D. Fernandez Espinosa, L. Romorini, et al., Specific preferences in lineage choice and phenotypic plasticity of glioma stem cells under BMP4 and noggin influence, Brain Pathol. 26 (1) (2016) 43–61.
[33] M. Tarragona, M. Pavlovic, A. Arnal-Estapé, J. Urosevic, M. Morales, M. Guiu M, et al., Identification of NOG as a specific breast cancer bone metastasis-supporting gene, J. Biol. Chem. 287 (25) (2012) 21346–21355.
[34] S.J. Lee, Y.J. Choi, H.I. Kim, H.E. Moon, S.H. Paek, T.Y. Kim, et al., Platycodin D inhibits autophagy and increases glioblastoma cell death via LDLR upregulation, Mol. Oncol. 16 (1) (2022) 250–268.